APWEN Journal of Engineering, Science and Technology
ISSN: 2714-2396, Volume 9 Issue 1

COMPARATIVE THERMAL RESPONSE ASSESSMENT OF STEEL AND CONCRETE BRIDGE GIRDERS UNDER ISO 834 FIRE EXPOSURE USING FINITE ELEMENT ANALYSIS

S.O. Oriakhi[1*], O.R. Ogirigbo[2]

[1] Department of Civil Engineering, University of Benin, P.M.B 1154, Ugbowo, Benin City, Edo State.
[2] Department of Civil Engineering, University of Benin, P.M.B 1154, Ugbowo, Benin City, Edo State.

Corresponding email: omosighoiyawe@gmail.com

Received: 28 April 2026 **Accepted**: Date 30 May 2026 **Published**: 16 June 2026

Abstract. Despite its well-known vulnerability to fires, there is little knowledge about the thermal behavior of bridge infrastructure under different configurations of girder sections. This paper conducts FE analysis of the comparison between the thermal behaviors of unprotected steel I-beam girders, concrete I-beam girders, and concrete rectangular beams when exposed to ISO 834 fire conditions. Specifically, 2D thermal FE models were made using ABAQUS to analyze how the heat is distributed within each section during 3600 seconds of fire exposure. The results reveal large variations in the heat resistance of each type of the section. Unprotected steel I-beams reached near total thermal saturation after only 1200 seconds, with temperatures reaching over 994ºC; in contrast, concrete sections showed good insulating ability, keeping their inner temperatures under 400ºC even after an hour. The remaining structural capacity can be estimated based on Eurocode reduction factors. For example, concrete rectangular beam will keep approximately 40% of its strength after 3600 seconds, whereas unprotected steel will only retain 4% of its original strength in the same duration. It should be emphasized here that the application of passive fire protection systems like intumescent coating and SFRM could dramatically increase the fire resistance of steel members. This is because materials have different properties which affect their thermal behaviors – steel with its high conductivity of 53.3 W/mK heats quickly and evenly, while concrete is slower and maintains larger thermal gradients.

Keywords: ABAQUS, Bridge Girders, Finite Element Analysis, Fire Resistance, Thermal Response.

1 Introduction

Bridge structures represent vital components of the transport infrastructure that are necessary for the functioning of economies, trades, and societies all over the world. Still, the risk associated with fires represents a danger to both structural stability, safety, and transport system functioning. Bridge fire can be caused by various factors, including crashes involving fuel-tankers, malfunctions of electrical equipment, arson, or wildfires (Peris-Sayol et al., 2017). The aim of this study was to use finite element modelling to evaluate the thermal behavioral response of different pedestrian bridge girder sections exposed to fire.

Despite the fact that structural steel is characterized by relatively high strength, it undergoes quick reduction in strength after reaching temperatures above 400ºC, and at temperatures around 550ºC retains only about 50% of its yield strength (Outinen and Mäkeläinen, 2004). Concrete shows less susceptibility to temperature changes and slow heat diffusion; still, its non-uniform structure makes it susceptible to complex damage patterns, which include explosive spalling due to moisture presence and strength degradation at temperatures over 600ºC (Kodur et al., 2017).

Geometry of girder cross-section affects fire resistance considerably. I-sections are effective load-bearing structures but their geometry allows for fast heat absorption, unlike rectangular profiles that show higher heat mass and low exposed surface areas and therefore provide better fire resistance(Gil, 2024). Nevertheless, there is a lack of systematic comparisons in terms of girder geometries.

1.1 Finite Element Modelling for Post-Fire Assessment of Bridge Structures

Finite Element Modelling (FEM) allows simulation of temperature effects on material characteristics, transient heat transfer, and damage formation throughout fire exposure, leading to a better assessment method. Examples of bridge fires in history include the fire of the Charilaos Trikoupis Bridge in 2005, the bridge collapse of I-75 Highway Bridge in 2009, and tanker explosion on the Apakun/Airport Bridge along the Oshodi-Apapa Expressway in Lagos in 2021 as shown in Fig 1. Such examples highlight the detrimental impacts of fire on the structure and show the importance of using better methods in evaluating the structural integrity of bridges after fire exposure (Godart et al., 2015).

Fig 1: Tanker Explosion Under Bridge in Lagos, Nigeria (Aliyu, A. 2021)

Many researchers have used FEM to perform post-fire structural analysis. For instance, Issa and Izadifard, (2021) performed the numerical simulation of the behavior of reinforced concrete beams at higher temperatures, obtaining excellent correlation with the experiments. Kodur and Dwaikat, (2008) built a finite element model to estimate the fire resistance of reinforced concrete beams.

Fig 2: Tanker Explosion at Mathilde Bridge (Godart et al., 2015)

Another example includes Hesien et al., (2025) who used FEM in the flat plates structure. Also to note the bridge fire in Pont Mathilde bridge in 2012, as shown in Fig 2.

This study by Peris-Sayol et al., (2017) as shown in Fig 3, compared different types of bridges under fire conditions. From their results, it can be seen that the most common bridges damaged due to fire were the composite deck bridges that contained steel girders and reinforced concrete slabs.

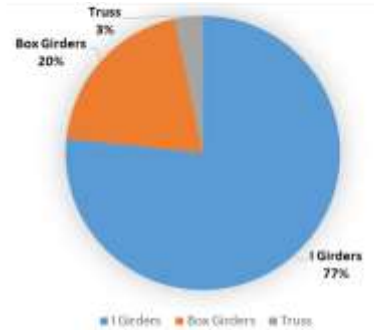

Fig 3: Percentage of Bridge Types Exposed to Fire (Peris-Sayol et al., 2017).

2 Methodology

2.1 Material Properties at Elevated Temperatures

2.1.1 Structural Steel

Structural steel shows extreme sensitivity to higher temperatures since the performance of the material worsens greatly with increasing temperature exposure. According to En, (2005)standards based on Eurocode 3, the yield strength of structural steel is fully preserved in an ambient temperature environment but reduces gradually to 78%, 47%, 23%, and 6% at 400ºC, 500ºC, 600ºC, and 800ºC, respectively, because higher atomic vibration makes metallic bonds more flexible. Elastic modulus also degrades in a similar fashion affecting the stiffness of the beam, and thermal conductivity varies from 53.3 W/mK to 27.3 W/mK between 20ºC and 800ºC.

2.1.2 Concrete

Concrete shows different reactions to temperature increases because of low thermal conductivity that ranges between 1.6 to 1.0 W/mK at 800ºC (Narayanan and Beeby, 2005). As a result, slow heating leads to high internal temperature gradients. Heat absorption capacity becomes greater in concrete as temperature rises; however, evaporated moisture inside delays internal heating (Asadi et al., 2018). Compressive strength decreases significantly from 300ºC but drops gradually to 75%, 45%, and 20% at 400ºC, 600ºC, and 800ºC. Explosive spalling due to increasing internal pore pressure from 300ºC to 800ºC exposes the reinforcement and accelerates deterioration (Amran et al., 2022).

2.2 Girder Geometry Specifications

2.2.1 Steel I-Beam Configuration

For analysis, a UKB 533 × 312 × 150 steel I-beam section, having a yield strength of 355 MPa according to the S355 specification standard (Fig 4), was selected. Properties of the steel section depend on temperature, allowing for consideration of temperature penetration and reactions. The density of steel was considered to be constant equal to 7850 kg/m³. According to the specific heat capacity, specified in Eurocode 3 standards, it was assumed to vary from 440 J/kg·K at 20ºC to 650 J/kg·K at temperatures exceeding 900ºC (with maximum at about 5000 J/kg·K near 735ºC) (Brown, 2018). Thermal conductivity decreased from 53.3W/mK at ambient to 27.3W/mK at temperatures exceeding 800ºC.

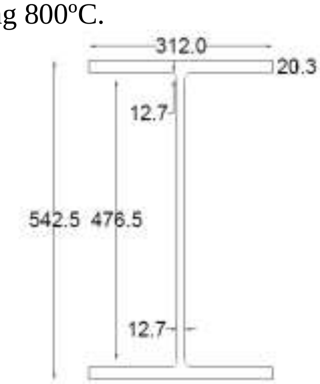

Fig 4: Geometry of Steel I Beam

2.2.2 Concrete I-Beam Configuration

The steel I-beam presented in Fig 5, was created in adherence to C35 grade of reinforced concrete and used reinforcement with yield strength of 460MPa and density of 2500kg/m³. Since only thermal response of the modelled beam was considered, there was no need to explicitly create reinforcement bars. Their temperatures were determined based on temperatures of surrounding concrete. As a result, concrete areas containing reinforcement were assumed to have similar properties as homogenous thermal material. This method is generally accepted in heat transfer simulations (Alain and Pierre, 2019).

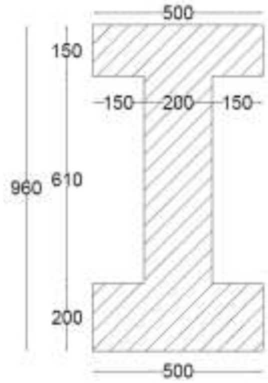

Fig 5: Geometry of Concrete I Beam

2.2.3 Concrete Rectangular Beam Configuration

Normal-weight concrete having density of 2500 kg/m³ was modelled using Eurocode 2 specifications on thermal properties of concrete used for creating rectangular concrete beam in Fig 6. Characteristic peaks of specific heat capacity related to moisture evaporation caused its values to change from 900J/kg·K at room temperature to 1000J/kg·K at 200ºC and 1100J/kg·K above 400ºC (Narayanan and Beeby, 2005). Thermal conductivity varied between 1.36W/m·K at 20ºC and 0.54 W/m·K at 1200ºC following the non-linear relationship of Eurocode 2.

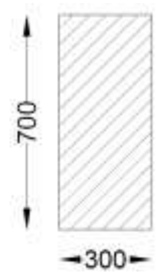

Fig 6: 2D Geometry of Rectangular Concrete Beam Dimension

2.3 ABAQUS Modeling

The sequence of ABAQUS modelling included eight successive stages – geometry creation, material property definition, step settings, loading boundary and initial conditions, imposition of fire loads, meshing, running thermal analysis and post-processing. The procedure began with geometry creation, where two dimensional cross-sections of steel I-beam, concrete I-beam and rectangular concrete beam were made as the simulation concerned heat transfer in the section plane (Piekarska et al., 2010). Thermal properties such as thermal conductivity, specific heat capacity and density were defined according to Eurocode standards (Neupane, 2020).

Step module was established in order to perform transient heat transfer analysis for 1200, 2400, and 3600 seconds and requests for output variables of nodal temperature, reaction flux and heat flux were set (Watson et al., 2012).

2.4 Boundary Conditions and Fire Exposure

The effects of fire on the structural system were simulated by thermal boundary conditions, which involved the heating of the bottom flange and web surfaces with initial conditions of ambient temperatures set to 20ºC, assuming that the top surfaces were insulated. The convection and radiation heat transfers occurred for exposed surfaces, whereby the following parameters were considered: film coefficient of 25 W/m²K, emissivity of 0.7, and Stefan–Boltzmann constant of 5.67×10^{-8} W/m²K⁴ while for non-exposed surfaces the film coefficient of 9 W/m²K was used (Cook, 2007).

The fire load was applied based on the ISO 834 cellulosic fire curve shown in Fig 7 and used the tabular amplitude definition such that ABAQUS could interpolate the temperature as a function of time for exposed surfaces using equation (1) where T refers to fire gas temperature (ºC) and t is time in minutes.

$$\boldsymbol{T = 20 + 345\, log_{10}(8t + 1)} \quad (1)$$

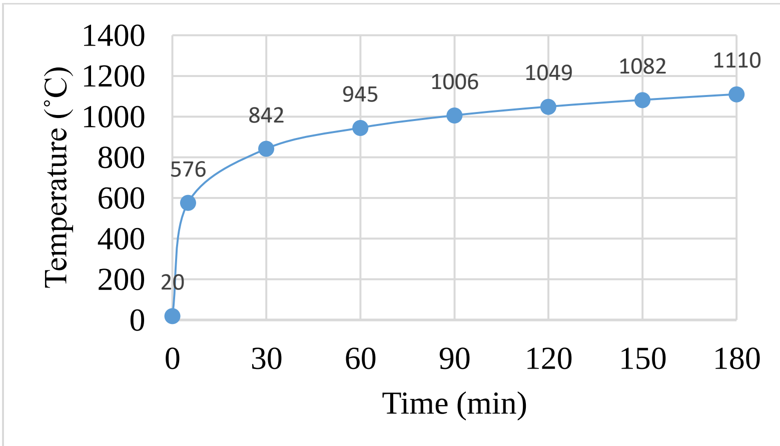

Fig 7: Standard Fire Curve (Cook and Cook, 2007)

2.5 Meshing and Heat Transfer

DC2D4 four-node bilinear heat transfer quadrilateral elements were used for modeling. Meshing for the steel I-beam, concrete I-beam, and rectangular beam was done using global seed sizes of 8, 15, and 10, respectively, to obtain more refined mesh distributions that would capture thermal gradients (Dal-Sasso et al., 2023). Time-stepping procedure was automated to ensure numerical stability, especially in the first few minutes of fast heating (Koric et al., 2009).

In order to study heat flow between different layers and analyze the time evolution of temperatures, a transient heat transfer analysis was used in place of the steady-state analysis. ABAQUS performs simulations of the heat transfer equations with regard to the material definitions, meshes, and fire boundary conditions specified earlier (Hodges et al., 2017). As a result, the heat transfer analyses generated temperature distribution patterns and other information about thermal gradients and heating rates, among others, which were extracted and organized for comparative evaluation for the three types of beams (Aliş et al., 2022).

3 Results and Discussion

3.1 Steel I-Beam Thermal Response

After 1200 seconds of exposure to fire based on the ISO 834 standard, significant thermal penetration was evident for the steel I-beam, with almost the entire cross-section being heated to relatively high temperatures, as can be seen in Fig 8. After 1200 seconds of fire, the bottom flange recorded 994ºC, the web 906ºC, and the top flange 640ºC. The high thermal conductivity and the low thermal mass of the material facilitated quick heating, small temperature gradients, and fast heat transfer within the section, thus illustrating its vulnerability without thermal insulation under severe fire conditions (Vácha et al., 2016).

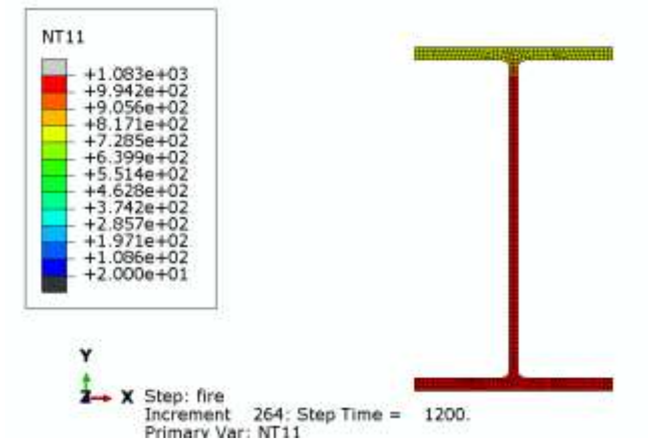

Fig 8: Nodal Temperature of Steel I-Beam at 1200seconds

At 2400 seconds, as illustrated in Fig 9, there is a near uniform distribution of temperature in the cross-section (thermal saturation, whereby the steel beam has saturated and cannot absorb more heat), with temperatures above 1040ºC and very small temperature differences.

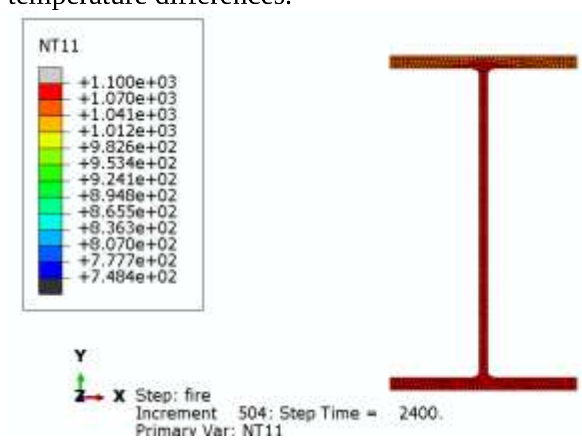

Fig 9: Nodal Temperature of Steel I-Beam at 2400seconds

Temperature values around 3600 seconds maintained a high degree of consistency, remaining at approximately 1010ºC, indicating prolonged exposure to very high heat and approaching thermal steady state as represented in Fig 10. These results are far higher than that critical temperature of steel, which is about 920ºC, where there is a drastic reduction in load carrying capacity (Wong, 2017). Thus, it was confirmed that unprotected steel beams are highly vulnerable under fire load.

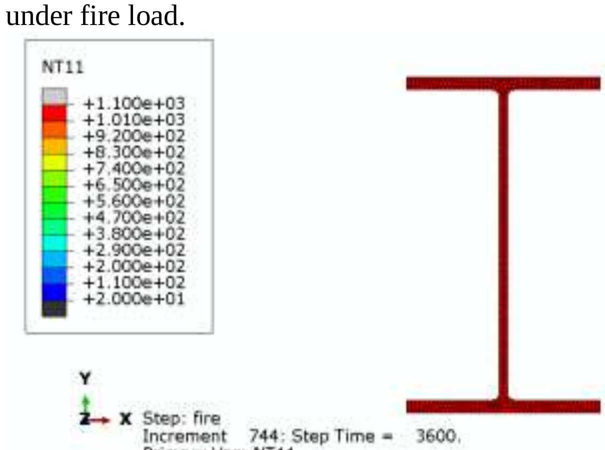

Fig 10: Nodal Temperature of Steel I-Beam at 3600seconds

3.2 Concrete I-Beam Thermal Response

3.2.1 Temperature Distribution

Thermal performance of concrete I-beams differed from that of steel. Temperatures exhibited great gradients across the sections of the beam. After 1200 seconds Fig 11, temperatures of the lower flange approached 821ºC while those of the upper flange remained much lower at around 400ºC. Temperatures of internal core were less than 600ºC.

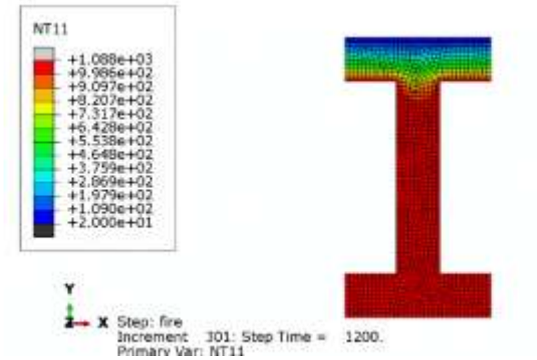

Fig 11: Nodal Temperature of Concrete I-Beam at 1200seconds

After 2400 seconds, surface temperatures increased to reach 830ºC, yet those of core did not go up much. This temperature distribution, shown in Fig 12, was similar to that after 1200 seconds. It should be noted that upper flanges did not exhibit any growth in temperatures due to their distance from fire and thermal insulation of other elements.

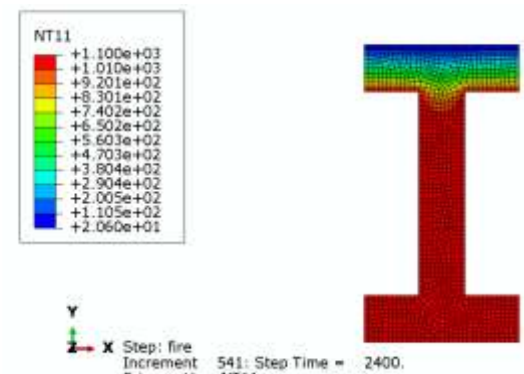

Fig 12: Nodal Temperature of Concrete I-Beam at 2400 seconds

After 3600 seconds (Fig 13) temperatures on the surfaces passed 1010ºC while those inside the section were still not higher than 700ºC.

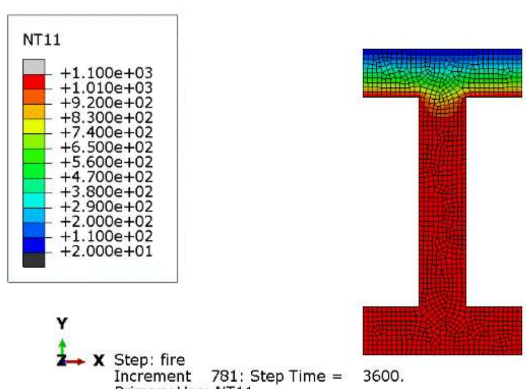

Fig 13: Nodal Temperature of Concrete I-Beam at 3600 seconds

3.2.2 Spalling Assessment

According to current temperature readings and literature review, spalling would begin during the analyzed time frame. As highlighted by Amran et al., (2022),), spalling begins at temperatures of about 300°C and increases significantly in intensity at temperatures between 600 and 800ºC. The lower flange and lower web zones, with temperatures higher than 820ºC for all analysis times, had high chances of spalling.

In this case, spalling would lower the cross-sectional area, make reinforcement directly susceptible to heat, and increase the rate of degradation. The slenderness of the web section (I-section with 150 mm) limits its thermal inertia and restricts evaporation routes, increasing the probability of spalling compared to thicker sections (Mohammed et al., 2022).

3.3 Concrete Rectangular Beam Thermal Response

3.3.1 Temperature Distribution

The result from all the tested sections showed that the rectangular concrete beam was most resistant to fire. With a temperature of 1200 seconds, as indicated in Fig 14, the bottom surface would reach temperatures of 910ºC, whereas the core temperature would stay below 376ºC. This gives a sharp thermal gradient due to both compactness and the material.

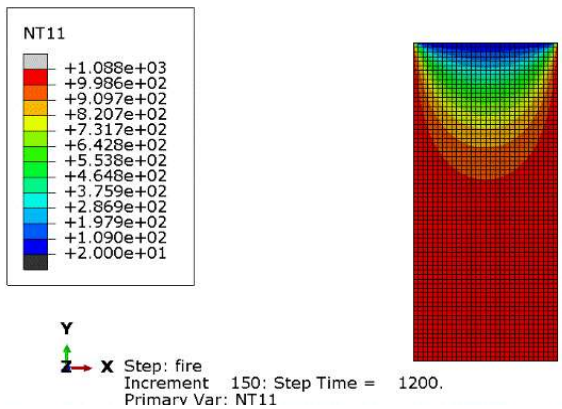

Fig 14: Nodal Temperature of Concrete Rectangular Beam at 1200 seconds

Improved fire resistance in case of concrete rectangles results from the following reasons: high cross-section area; deeper core; and smaller surface area. Such features enable better heat accumulation, thus protecting inner areas from excessive thermal impact. In combination with poor thermal conductivity of concrete material, such properties ensure much more efficient fire resistance compared to I-beams (Gil, 2024).

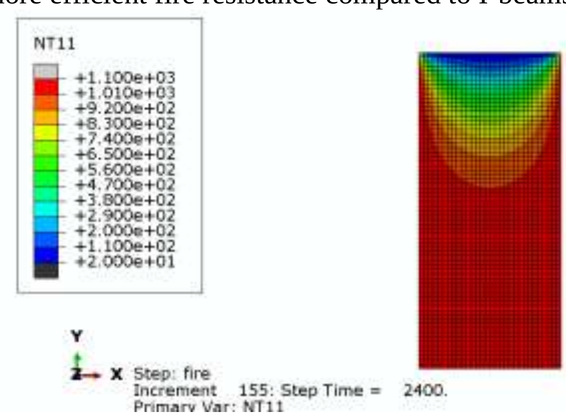

Fig 15: Nodal Temperature of Concrete Rectangular Beam at 2400 seconds

At 2400 seconds, the core showed temperatures only up to 200ºC despite temperatures near 920ºC at the surface (Fig 15), which shows considerable thermal lagging. At 3600 seconds (Fig 16), despite extreme temperatures of over 1010ºC at the exposed surfaces, significant portions were still under critical values for reduction in strength of reinforcement, showing that considerable residual capacity is preserved.

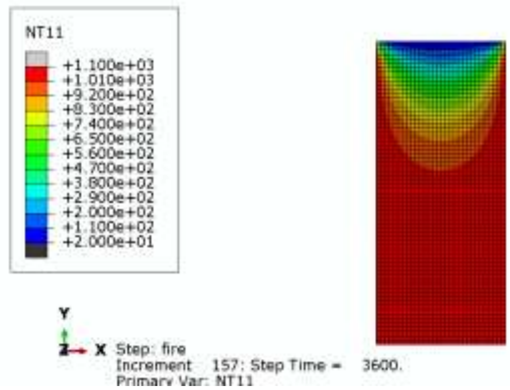

Fig 16: Nodal Temperature of Concrete Rectangular Beam at 3600 seconds

3.3.2 Reduced Spalling Vulnerability

The rectangle shape provided certain resistance against spalling because the bigger cross-section area allowed the section to have higher thermal mass, resulting in slower heating rates and smaller thermal stresses. Lower perimeter-to-area ratios also decreased the share of the cross-section area affected by strong spalling due to surface degradation (Winful, 2018). Thermal cracks and surface spalling were present, but their intensity is expected to be less compared to that for I-beams. It could result in penetration depths only 20-30 mm into concrete surface layers.

3.4 Residual Strength Assessment

3.4.1 Steel I-Beam Residual Capacity

The steel I-beam shows severe reduction of its strength throughout the range of the considered times exposed to fire. At a time of 1200 seconds, where the mean temperature of the cross-section reaches 994ºC, the Eurocode 3 reduction factor is equivalent to a strength retention of 0.36, meaning that the initial yield strength of 355 MPa is reduced to 129 MPa. At a period of 2400 seconds (1041ºC), the retention of strength reduces to 0.038 (3.8%), thus giving a residual strength of 13.5 MPa. By 3600 seconds (1010ºC), strength retention will be around 0.04 (4%), with residual strength being 15 MPa.

3.4.2 Concrete I-Beam Residual Capacity

The reinforced concrete beam shows more capacity retention than the steel one, but also experiences considerable degradation. At 1200 seconds, where the temperature of the reinforcements reaches 821ºC, the reduction factor is equivalent to a strength retention of 0.70, indicating that the initial yield strength of 460 MPa is reduced to 322 MPa. At 2400 seconds (830ºC), the strength retention would be 0.40 (40%), implying a residual strength of 184 MPa. By 3600 seconds at 1010ºC, the retention will be 0.25.

3.4.3 Concrete Rectangular Beam Residual Capacity

The rectangular concrete beam demonstrated outstanding strength retention throughout all intervals of time tested. With a core temperature at 376°C at 1200 seconds, 0.74 or 74% capacity retention resulted in a capacity of 340.4 MPa from an initial capacity of 460 MPa. After 2400 seconds when the core temperature was at 200ºC, capacity retention was still 0.50 (50%), leading to a capacity of 230 MPa. At a later period of 3600 seconds and core temperatures estimated at 400ºC, 0.40 (40%) strength retention led to a capacity of 184 MPa.

3.5 Comparative Strength Analysis

Comparing the performances of the three types of girders showed significant differences, due to the materials used and geometrical configuration of the structures. While steel I-beam could maintain only 4% of its capacity after one hour, the concrete I-beam managed 25% capacity retention while the rectangular concrete beam had a strength retention of 40%. Rectangular section showed 15% higher capacity than the I-beams due to the difference in geometry.

3.6 Validation Against Established Research

3.6.1 Steel I-Beam Validation

Thermal resistance properties predicted for steel I-beams correlated well with the literature and design code provisions. Eurocode 3 predictions for unprotected steel indicate rapid increase of temperature to a critical point of 15-20 minutes, with an expected temperature close to 1000ºC reached within 1200 seconds. This is explained by the high thermal conductivity of steel, confirmed by similar fire tests performed on steel members (Issa and Izadifard, 2021).

The predictions for the residual strength after 1200 seconds indicating 36% strength retention corresponded to the predictions of Eurocode, where steel has a strength retention between 30 and 40 percent at 600ºC. The rapid strength loss of 3-4 percent after 2400-3600 seconds corresponds to the information presented in literature according to which steel loses up to 90% strength capacity above 750-800ºC (Brown, 2018).

3.6.2 Concrete I-Beam Validation

Temperature distribution in the concrete I-beam showed that the outer layers had high temperatures, more than 800ºC, whereas the inner parts were cooler, with less than 400ºC at 1200 s. These results are consistent with current understanding of the heat transfer properties of concrete structures in fire (Asadi et al., 2018). Large thermal gradients due to low thermal conductivity of concrete have been reported in the fire engineering literature.

Predicted spalling above 300ºC agrees with findings reported by Amran et al., (2022), where the same threshold is cited as an indicator of fire initiation. Estimated residual strengths of 70% and 25% at 1200 s and 3600 s respectively agree with concrete fire behavior. Literature shows that, under standard conditions, concrete can retain 65% to 75% of strength when heated initially but reduces to 35% to 45% after some time and 20% to 30% after 1 hour (Golewski, 2023).

3.6.3 Rectangular Beam Validation

The rectangular beam performed well in terms of temperature resistance since it was able to keep its inner temperature at below 400ºC even after 3600 s exposure. This is in line with fire resistance of massive cross-section beams since the thermal resistance increases in relation to increased size (Kamil et al., 2019). In addition, large temperature gradients of about 534ºC in 75 mm of thickness are expected in compact beams with exposed surfaces.

Estimated residual strength of 74% retention after 1200 s exposure and 40% after 3600 s matches with massive concrete literature. Compact geometries are known to show high structural resistance due to low surface area to volume ratio. Gil, (2024) explains that differences in resistance up to 15% can be expected depending on geometry and cross-sectional dimensions.

4 Conclusion

In comparison to unprotected steel, concrete showed noticeably better resistance to ISO 834 fire exposure. At one-hour time exposure, concrete members maintained approximately 25-85% of the initial load capacity, while unprotected steel retained only 4-15% of the initial capacity. The difference can be explained by the lower thermal conductivity coefficient of concrete and the ability of concrete to maintain its strength properties even in a state of elevated temperature. The heating of steel I-beams was extremely fast, and after 1200 seconds, the near-uniform heating of steel was reached, exceeding 990ºC, causing the destruction of steel by the end of one hour.

Concrete girders showed slower heating, and the presence of thermal gradient helped them withstand higher temperatures due to the protection of core regions and reinforcing bars. Concrete I-beams were able to maintain approximately 70% of initial capacity after 1200 seconds, while rectangular cross-sections showed better results with 74% and 40% initial capacity after 1200 seconds and 3600 seconds respectively. The advantage of rectangular cross-sections is due to the high thermal mass, compact shape, and low ratio of the external surface area to volume. In addition, temperature distribution showed that cores of rectangular beams had much lower temperature than cores of I-beams for similar duration of fire exposure.

Destruction mechanisms for the two materials differed considerably from each other. While the rapid heating of steel led to the loss of strength properties and complete failure after 30-40 minutes of the process, the damage for concrete included such mechanisms as cracking, spalling, chemical reactions, and was more focused on surface regions with the protection of core regions. Validation of the model showed a good correlation of results obtained through simulation with Eurocode requirements and experimental data.

Acknowledgment

Sincere gratitude and appreciation will be given to Engr. Dr. Iziengbe Inerhunwa for his invaluable guidance and technical expertise all through the course of this research.

References

Alain, M., Pierre, P., 2019. Modelling of concrete behaviour at high temperature.

Aliş, B., Yazici, C., Mehmet Özkal, F., 2022. Investigation of Fire Effects on Reinforced Concrete Members via Finite Element Analysis. ACS Omega 7, 26881–26893. https://doi.org/10.1021/acsomega.2c03414

Aliyu, A. (2021, January 12). Tanker explosion: Lagos bridge remains closed as repair work begins. *Daily Trust*. https://dailytrust.com/tanker-explosion-lagos-bridge-remains-closed-as-repair-work-begins/

Amran, M., Huang, S.-S., Onaizi, A.M., Murali, G., Abdelgader, H.S., 2022. Fire spalling behavior of high-strength concrete: A critical review. Constr. Build. Mater. 341, 127902.

Asadi, I., Shafigh, P., Hassan, Z.F.B.A., Mahyuddin, N.B., 2018. Thermal conductivity of concrete–A review. J. Build. Eng. 20, 81–93.

Awoyera, P.O., Naser, M.Z., 2024. Construction Materials and Their Properties for Fire Resistance and Insulation. Elsevier.

Brown, D., 2018. Eurocode 3: Design of steel structures. Des. Struct. Elem. 95, 38–38.

Cook, N., 2007. Designers' Guide to EN 1991-1-4 Eurocode 1: Actions on structures, general actions part 1-4. Wind Actions 66–67.

Cook, N., Cook, N.J., 2007. Designers' Guide to EN 1991-1-4 Eurocode 1: Actions on structures, general actions part 1-4. Wind actions. https://doi.org/10.1680/dgte1.31524

Dal-Sasso, M.F., Assis, L.S. de, Farage, M.C.R., Bastos, F. de S., Beaucour, A.-L., 2023. Numerical evaluation of aggregate size influence on concrete mechanical damage under high temperatures. Rev. IBRACON Estrut. E Mater. 16, e16605.

En, C., 2005. 1-2, Eurocode 3: Design of steel structures, Part 1.2: General rules–Structural fire design. Bruss. Belg. Com. Eur. Norm.

Gil, A.M., 2024. Response of Fire Exposed Concrete Bridge Girders. Michigan State University.

Godart, B.F., Berthellemy, J., Lucas, J.P., 2015. Diagnosis, Assessment and Repair of the Mathilde Bridge Close to Collapse during a Fire. Struct. Eng. Int. 25, 331–338. https://doi.org/10.2749/101686615X14210663188691

Golewski, G.L., 2023. The phenomenon of cracking in cement concretes and reinforced concrete structures: the mechanism of cracks formation, causes of their initiation, types and places of occurrence, and methods of detection—a review. Buildings 13, 765.

Hesien, M., Youssef, M.A., El-Fitiany, S., 2025. Finite element analysis of flat plate structures in fire. Fire 8, 252.

Hodges, J., Rippe, C., Case, S.W., Lattimer, B.Y., 2017. Predicting the structural response of a compartment fire using full-field heat transfer measurements. Fire Saf. J. 91, 471–479.

Issa, C.A., Izadifard, R.A., 2021. Numerical simulation of the experimental behavior of RC beams at elevated temperatures. Adv. Model. Simul. Eng. Sci. 8, 12. https://doi.org/10.1186/s40323-021-00198-1

Kamil, G.M., Liang, Q.Q., Hadi, M.N., 2019. Numerical analysis of axially loaded rectangular concrete-filled steel tubular short columns at elevated temperatures. Eng. Struct. 180, 89–102.

Kodur, V., Hibner, D., Agrawal, A., 2017. Residual response of reinforced concrete columns exposed to design fires. Procedia Eng. 210, 574–581.

Kodur, V.K.R., Dwaikat, M., 2008. A numerical model for predicting the fire resistance of reinforced concrete beams. Cem. Concr. Compos. 30, 431–443.

Koric, S., Hibbeler, L.C., Thomas, B.G., 2009. Explicit coupled thermo-mechanical finite element model of steel solidification. Int. J. Numer. Methods Eng. 78, 1–31. https://doi.org/10.1002/nme.2476

Mohammed, H., Ahmed, H., Kurda, R., Alyousef, R., Deifalla, A.F., 2022. Heat-induced spalling of concrete: A review of the influencing factors and their importance to the phenomenon. Materials 15, 1693.

Narayanan, R.S., Beeby, A.W., 2005. Designers' Guide to EN 1992-1-1 and EN 1992-1-2. Eurocode 2: Design of Concrete Structures: General Rules and Rules for Buildings and Structural Fire Design. Thomas Telford London.

Neupane, D., 2020. Structural analysis technique of simple steel structures exposed in fire using ABAQUS.

Outinen, J., Mäkeläinen, P., 2004. Mechanical properties of structural steel at elevated temperatures and after cooling down. Fire Mater. 28, 237–251. https://doi.org/10.1002/fam.849

Peris-Sayol, G., Paya-Zaforteza, I., Balasch-Parisi, S., Alós-Moya, J., 2017a. Detailed Analysis of the Causes of Bridge Fires and Their Associated Damage Levels. J. Perform. Constr. Facil. 31, 04016108. https://doi.org/10.1061/(ASCE)CF.1943-5509.0000977

Piekarska, W., Kubiak, M., Saternus, Z., 2010. Application of Abaqus to analysis of the temperature field in elements heated by moving heat sources. Arch. Foundry Eng. 10, 177–182.

Vácha, J., Kyzlík, P., Both, I., Wald, F., 2016. Beams with corrugated web at elevated temperature, analytical and numerical models for heat transfer. Fire Saf. J. 86, 83–94.

Watson, K.A., Brown, A.O., Hackett, R.K., Pham, A., 2012. Finite element analysis learning modules for an undergraduate heat transfer course: implementation and assessment, in: 2012 ASEE Annual Conference & Exposition. pp. 25–638.

Winful, D.A.A.A., 2018. Structural fire design considerations for high strength steel (PhD Thesis). Brunel University London.

Wong, M.B., 2017. Temperature analysis of partially heated steel members in fire. J. Constr. Steel Res. 128, 1–6.